

MIT Open Access Articles

Cathode buffer layers based on vacuum and solution deposited poly(3,4-ethylenedioxythiophene) for efficient inverted organic solar cells

The MIT Faculty has made this article openly available. **Please share** how this access benefits you. Your story matters.

Citation: Barr, Miles C., Chiara Carbonera, Riccardo Po, Vladimir Bulovic#, and Karen K. Gleason. "Cathode buffer layers based on vacuum and solution deposited poly(3,4-ethylenedioxythiophene) for efficient inverted organic solar cells." *Applied Physics Letters* 100, no. 18 (2012): 183301. © 2012 American Institute of Physics

As Published: <http://dx.doi.org/10.1063/1.4709481>

Publisher: American Institute of Physics (AIP)

Persistent URL: <http://hdl.handle.net/1721.1/79730>

Version: Final published version: final published article, as it appeared in a journal, conference proceedings, or other formally published context

Terms of Use: Article is made available in accordance with the publisher's policy and may be subject to US copyright law. Please refer to the publisher's site for terms of use.



Cathode buffer layers based on vacuum and solution deposited poly(3,4-ethylenedioxythiophene) for efficient inverted organic solar cells

Miles C. Barr, Chiara Carbonera, Riccardo Po, Vladimir Bulović, and Karen K. Gleason

Citation: *Appl. Phys. Lett.* **100**, 183301 (2012); doi: 10.1063/1.4709481

View online: <http://dx.doi.org/10.1063/1.4709481>

View Table of Contents: <http://apl.aip.org/resource/1/APPLAB/v100/i18>

Published by the [American Institute of Physics](#).

Additional information on Appl. Phys. Lett.



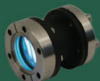



Journal Homepage: <http://apl.aip.org/>

Journal Information: http://apl.aip.org/about/about_the_journal

Top downloads: http://apl.aip.org/features/most_downloaded

Information for Authors: <http://apl.aip.org/authors>

ADVERTISEMENT

a sampling of our products		for surface and materials science	www. rbdinstruments .com	celebrating over 20 years of innovation
 deposition tools	 desorption systems	 sputter ion sources	 viewports	 usb picoammeters

Cathode buffer layers based on vacuum and solution deposited poly(3,4-ethylenedioxythiophene) for efficient inverted organic solar cells

Miles C. Barr,¹ Chiara Carbonera,² Riccardo Po,² Vladimir Bulović,³ and Karen K. Gleason^{1,a)}

¹*Department of Chemical Engineering, Massachusetts Institute of Technology, Cambridge, Massachusetts 02139, USA*

²*Centro ricerche per le energie non convenzionali, Istituto ENI Donegani, ENI S.p.A., Novara 28100, Italy*

³*Department of Electrical Engineering, Massachusetts Institute of Technology, Cambridge, Massachusetts 02139, USA*

(Received 12 February 2012; accepted 15 April 2012; published online 30 April 2012)

Vacuum and solution processed versions of poly(3,4-ethylenedioxythiophene) (PEDOT) are used as cathode interlayers in inverted organic photovoltaic cells comprising tetraphenyldibenzoperiflanthene as the electron donor and C₆₀ as the electron acceptor. Chemical treatment of the as-deposited PEDOT layers with tetrakis(dimethylamino)ethylene or cesium carbonate reduces the work function by up to 0.8 eV. Inserting these PEDOT layers at the indium tin oxide cathode results in improved electron collection and efficiencies of up to $2.3 \pm 0.2\%$, approaching the $3.2 \pm 0.3\%$ of the conventional device. This illustrates the potential for efficient polymer cathode materials and inverted device architectures compatible with either solution or vacuum processing. © 2012 American Institute of Physics. [<http://dx.doi.org/10.1063/1.4709481>]

Organic photovoltaic cells (OPVs) have received significant interest for their potential as a low-cost energy source, and efficiencies have recently reached records nearing 10% using both solution and vacuum deposition methods.¹ In the conventional orientation, the OPV is illuminated through a transparent hole-collecting anode deposited on the substrate, [e.g., indium tin oxide (ITO)], and electrons are collected by a low work function (LWF) metal cathode top contact. Development of efficient inverted device structures (i.e., electrons collected by a transparent cathode) would (1) provide more degrees of freedom in designing OPV fabrication schemes, including tandem and semitransparent devices,^{2–4} (2) allow for protection of the delicate organic semiconductor layers below metal oxide anodic buffer layers (e.g., MoO₃) prior to subsequent top layer deposition steps,^{5,6} and (3) are proposed to be more stable by allowing use of higher work function metal top contacts (e.g., Au or Ag)⁷ and protecting the air-sensitive electron acceptor layer (e.g., C₆₀).⁸ However, due to the high work function of common transparent conductors (e.g., ITO and conductive polymers) such structures require a readily processable LWF interfacial cathode buffer layer to provide sufficient electric field through the device and allowing for ohmic contact with the adjacent electron acceptor.^{4,7,9}

In this letter, we explore the use of poly(3,4-ethylenedioxythiophene) (PEDOT) deposited by both solution and vacuum deposition methods as a cathode buffer layer in inverted organic solar cells on ITO. The solution deposited version doped with poly(styrenesulfonate) (PEDOT:PSS) has been widely used as a hole-transporting anode buffer layer on ITO,^{9,10} and high-conductivity analogues have been proposed for use as the OPV anode^{3,11,12} or cathode.^{3,13} Similarly, vacuum-deposited PEDOT, in which the polymer film

is formed directly on the substrate by oxidative polymerization of vapor-phase precursors, has been explored for use as an anodic buffer layer,^{14,15} anode,^{14,16,17} and cathode.¹⁵ However, there have been few reports of PEDOT as a cathode buffer layer, due to its high work function.¹⁸ It has previously been shown that the organic reductant tetrakis(dimethylamino)ethylene (TDAE) lowers the work function of PEDOT:PSS (Ref. 19) and vapor-deposited PEDOT,²⁰ however, these layers were not incorporated in an OPV device. Similarly, cesium carbonate (Cs₂CO₃) has been demonstrated to lower the work function of ITO electrodes by both vacuum thermal evaporation and solution casting.^{5,9,21} Here, we incorporate PEDOT:PSS and vacuum deposited PEDOT treated with TDAE or Cs₂CO₃ as cathode interlayers in inverted OPVs on ITO, which we demonstrate improves electron collection efficiency compared to devices with no cathode buffer layer.

PEDOT films were deposited onto ITO-coated glass substrates (Kintec Co., sheet resistance = 15 Ω/sq) that were first solvent-cleaned and treated with O₂-plasma. The vapor-deposited PEDOT was deposited in a vacuum chamber using the oxidative chemical vapor deposition (oCVD) process,^{14,22} at 0.1 Torr and a substrate temperature of 80 °C via simultaneous exposure to vapors of 3,4-ethylenedioxythiophene monomer (Aldrich 97%, ~5 sccm) and sublimed FeCl₃ oxidant (Aldrich) for 2 min. The PEDOT:PSS (CLEVIOS™ P VP AI 4083) was filtered (0.45 μm), spin-coated at 4000 rpm for 60 s, and annealed at 200 °C for 5 min in air. Resulting film thicknesses were ~20 nm for oCVD PEDOT and ~50 nm PEDOT:PSS, measured by profilometer (Tencor P-16). Sets of both PEDOT films were then either (1) treated with liquid TDAE in nitrogen atmosphere for 60 s before spinning dry at 5000 rpm and transferring into vacuum or (2) coated with ~1 nm of Cs₂CO₃ via vacuum thermal evaporation. Work function measurements were performed in nitrogen

^{a)}Electronic mail: kkg@mit.edu.

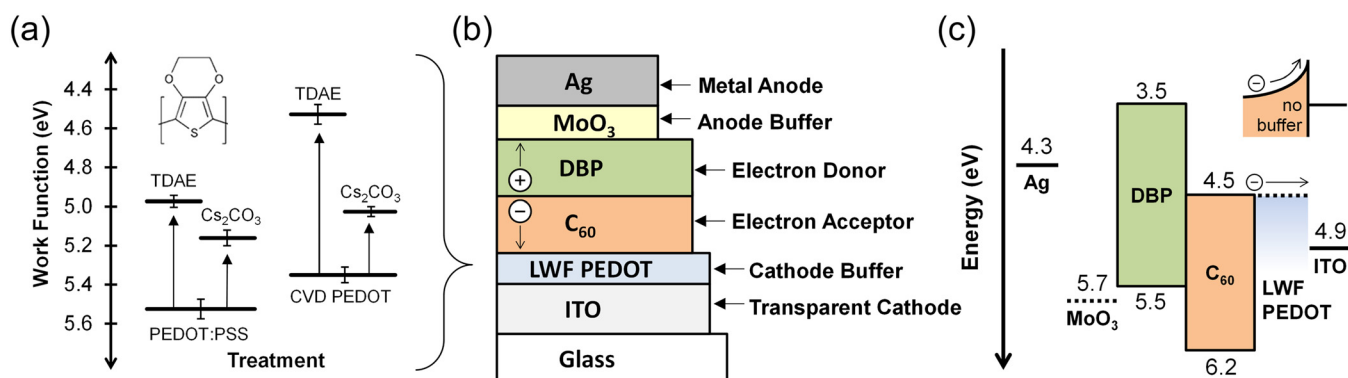


FIG. 1. (a) Work function of both PEDOT:PSS and CVD PEDOT treated with TDAE or Cs₂CO₃. (b) Schematic of the inverted device architecture with transparent ITO cathode and low work function PEDOT buffer layer inserted between ITO/C₆₀ interfaces. (c) Flat band energy level diagram for the inverted device architecture. The top-right inset shows the proposed electron-limiting Schottky barrier formed at an unbuffered ITO/C₆₀ interface. Band energies are taken from the literature.

atmosphere with a Scanning Kelvin Probe (SKP5050, KP Technology Ltd.) using a 2 mm gold tip, and were calibrated relative to a gold reference surface assumed to be 5.1 eV, which was measured before and after each sample and was stable over the course of the experiment. Average and standard deviation values were calculated from a scan of 220 points recorded evenly across a 1 cm² surface. OPVs were then fabricated using a bilayer heterojunction structure of C₆₀ (Aldrich, sublimed) as the electron acceptor and tetraphenyl-dibenzoperiflanthene (DBP, Lumtec) as the electron donor,²³ with an MoO₃ anode buffer layer and Ag top electrode. The DBP and C₆₀ were first purified once by thermal gradient sublimation, and then the OPV layers were sequentially deposited onto the ITO substrates (with and without the various PEDOT buffer layers) by thermal evaporation at $<10^{-6}$ Torr and rates of 0.1 nm s⁻¹. Shadow masks were used to define a 1 mm by 1.2 mm active device area. The resulting device structures were ITO, MoO₃ (20 nm), DBP (25 nm), C₆₀ (40 nm), Ag (conventional orientation) and ITO, (PEDOT), C₆₀ (40 nm), DBP (XX nm), MoO₃ (20 nm), Ag (inverted orientation). Current density-voltage (J-V) characteristics were measured in nitrogen atmosphere under simulated AM1.5G illumination from a 1 kW xenon arc-lamp (Newport 91191). Optical interference modeling was performed using transfer matrix formalism,²⁴ with exciton diffusion lengths $L_D^{C60} = 20$ nm and $L_D^{DBP} = 5$ –20 nm, and optical constants measured by variable angle spectroscopic ellipsometry (J. A. Woollam M-2000 S).

Figure 1(a) shows the change in work function measured for PEDOT:PSS and oCVD PEDOT films on ITO before and after treatment with TDAE and Cs₂CO₃. The decrease in work function upon treatment with liquid TDAE is ~ 0.6 eV with PEDOT:PSS (5.52 ± 0.05 eV to 4.97 ± 0.03 eV) and ~ 0.8 eV for the oCVD PEDOT (5.35 ± 0.04 eV to 4.53 ± 0.05 eV). The observed decreases in work function are consistent with the trends observed previously for TDAE with PEDOT and ITO.^{19,20,25} Previous reports for oCVD PEDOT showed that lowering the substrate temperature used during the deposition resulted in a 0.3 eV higher work function; thus, the change here suggests that the oCVD PEDOT can be modified by over 1 eV through a combination of deposition conditions and chemical treatment. The change in surface work function observed upon evaporation of Cs₂CO₃ was ~ 0.3 eV for both the PEDOT:PSS (5.52 ± 0.05 eV to

5.16 ± 0.04 eV) and oCVD PEDOT (5.35 ± 0.04 eV to 5.03 ± 0.03 eV) films. We note that the values observed for the as-deposited PEDOT:PSS and CVD PEDOT as much as ~ 0.2 eV higher than previously reports;^{22,26} which is most likely explained by different conditions and techniques used, as the kelvin probe and ultraviolet photoelectron spectroscopy measurements are highly sensitive to environmental conditions.²⁷

The ability to decrease the work function of the various PEDOT surfaces motivates their incorporation as cathode layers for electron collection in OPVs. Fig. 1(b) shows the schematic of inverted OPVs used here, in which the LWF PEDOT layer is inserted between the transparent ITO electrode and the adjacent C₆₀ electron acceptor. In the inverted orientation, the ITO collects electrons and the Ag collects holes. Fig. 1(c) shows the flat band energy level diagram for the inverted device, with the proposed LWF PEDOT layer raising the ITO cathode work function closer to the lowest unoccupied energy level (LUMO) of the C₆₀ layer and the MoO₃ layer raising the work function of the Ag anode towards the highest occupied energy level (HOMO) of the DBP layer.

The J-V characteristic of devices with and without the LWF PEDOT buffer layers are shown in Figure 2. Devices utilizing an unmodified ITO cathode and as-deposited CVD PEDOT and PEDOT:PSS cathode layers show a distinct “S” shape at reverse bias, suggesting the presence of a Schottky junction at the cathode contact in opposition to the diode formed at the DBP/C₆₀ heterojunction interface, which would create a barrier to electron collection (Fig. 1(c), inset).²⁸ This is evident in the J-V curve by the poor fill factor (FF) (0.37, 0.48, and 0.25, respectively) and reduced open-circuit voltage (V_{oc}) (0.79 V, 0.83 V, and 0.55 V, respectively) relative to the conventional device orientation (FF = 0.62 and V_{oc} = 0.91 V) with identical layer thicknesses. Replacing the as-deposited PEDOT layers with the LWF versions [Fig. 2(b)] results in improved FF (0.48, 0.57, 0.62, and 0.58, respectively) and V_{oc} (0.74 V, 0.84 V, 0.90 V, and 0.90 V, respectively) comparable to the conventional device ((FF = 0.62 and V_{oc} = 0.91 V). This high V_{oc} is supported by sufficient work function offset between the high work function MoO₃ layer at the anode²⁹ and the LWF PEDOT layer at the cathode.

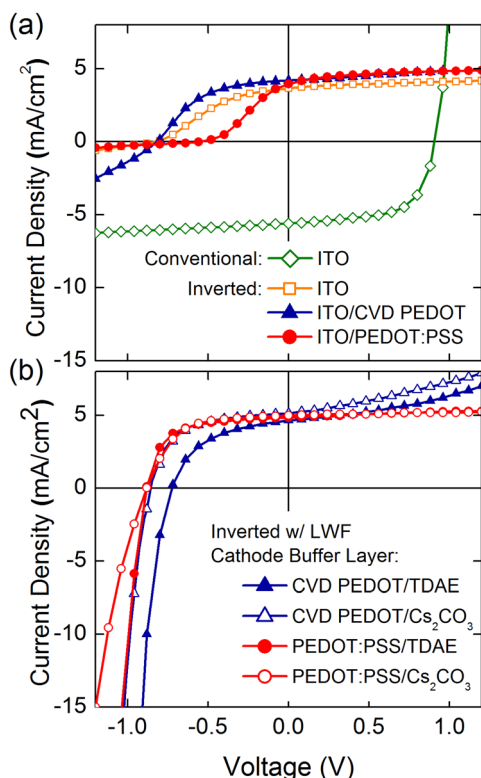


FIG. 2. J-V curves under AM1.5G simulated solar illumination. (a) Comparison of the conventional device orientation (ITO/MoO₃ 20 nm/DBP 25 nm/C₆₀ 40 nm/Ag) (open diamonds) with the same device stack inverted (ITO cathode) with no buffer layer on the ITO (open squares), and with untreated PEDOT layers on the ITO (filled triangles—CVD PEDOT, filled circles—PEDOT:PSS). (b) The same inverted device structure incorporating a LWF PEDOT buffer layer on the ITO cathode: CVD PEDOT/TDAE (filled triangles), CVD PEDOT/Cs₂CO₃ (open triangles), PEDOT:PSS/TDAE (filled circles), and PEDOT:PSS/Cs₂CO₃ (open circles).

We then optimize this inverted device structure using the PEDOT:PSS/TDAE cathode buffer layer by varying the DBP thickness (Fig. 3), subsequently moving the position of the reflective Ag interface relative to the DBP/C₆₀ interface. The structure is optimized at a DBP thickness of ~ 10 nm, corresponding to short-circuit current (J_{sc}) = 4.6 mA/cm², and maxima in V_{oc} = 0.89 V, FF = 0.6, and power efficiency (η_p) = 2.5%. The observed optimum J_{sc} is consistent with simulations modeling the optical interference of light inside the device with light reflected by the Ag anode,²⁴ and corresponds to a DBP exciton diffusion length (L_D^{DBP}) between 10 and 15 nm (Fig. 3, dashed lines). For this donor/acceptor pair, the optimal photocurrent is lower for the inverted structure than the conventional structure, because the short wavelength absorber (C₆₀, peak < 400 nm) is positioned farther from the reflective node, while the long wavelength absorber (DBP, peak ~ 610 nm) is closer to the reflective node, creating a mismatch in the positioning of the peak-wavelength optical electric field maxima within the respective layers. With bulk heterojunction structures, and donor/acceptor pairs with different peak absorption characteristics, higher efficiencies should be possible with such inverted OPVs.

In conclusion, we have demonstrated the use of vacuum and solution deposited low work function PEDOT cathode buffer layers. Incorporation of these materials at the cathode in inverted DBP/C₆₀ heterojunction OPVs prevents the for-

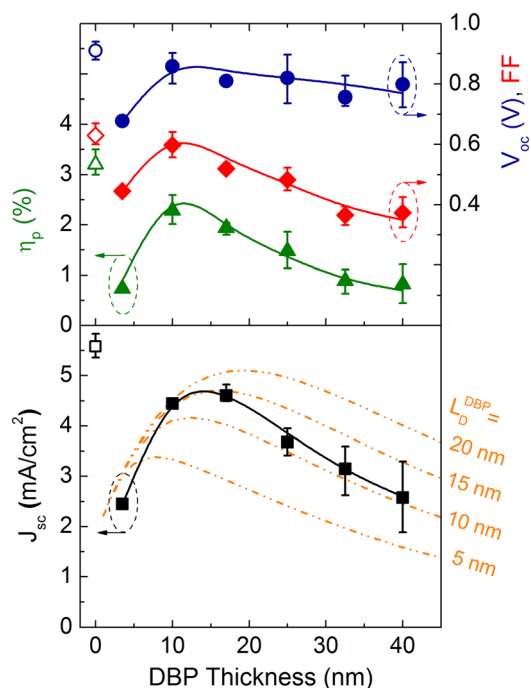


FIG. 3. Power conversion efficiency, η_p (filled triangles), open-circuit voltage (filled circles), fill-factor (filled diamonds), and short-circuit current (filled squares) as a function of the DBP electron donor layer thickness for the inverted device with PEDOT:PSS/TDAE buffer layer. The dashed lines show short-circuit current vs. DBP thickness calculated from optical interference simulations using DBP exciton diffusion lengths from 5 to 20 nm (as noted). The control cell in the conventional orientation (ITO/MoO₃ 20 nm/DBP 25 nm/C₆₀ 40 nm/Ag) is included as x = 0 for reference (open symbols). Solid lines are to guide the eyes.

mation of an electron-limiting Schottky junction at the cathode in opposition to the diode formed by the DBP/C₆₀ heterojunction, thereby increasing FF and V_{oc} relative to cells with an improperly or un-buffered cathode interface. We find an optimal efficiency of 2.5% using an inverted DBP/C₆₀ heterojunction structure. This illustrates the potential for efficient polymer cathode materials and inverted device architectures compatible with solution and vacuum processing.

This work was supported by Eni S.p.A. under the Eni-MIT Alliance Solar Frontiers Program and by a National Science Foundation Graduate Research Fellowship.

- ¹M. E. Alf, A. Asatekin, M. C. Barr, S. H. Baxamusa, H. Chelawat, G. Ozaydin-Ince, C. D. Petruczuk, R. Sreenivasan, W. E. Tenhaeff, N. J. Trujillo, S. Vaddiraju, J. Xu, and K. K. Gleason, *Adv. Mater.* **22**, 1993 (2010).
- ²C. Waldauf, M. Morana, P. Denk, P. Schilinsky, K. Coakley, S. A. Choulis, and C. J. Brabec, *Appl. Phys. Lett.* **89**, 233517 (2006).
- ³S. K. Hau, H.-L. Yip, J. Zou, and A. K. Y. Jen, *Org. Electron.* **10**, 1401 (2009).
- ⁴L.-M. Chen, Z. Hong, G. Li, and Y. Yang, *Adv. Mater.* **21**, 1434 (2009).
- ⁵G. Li, C. W. Chu, V. Shrotriya, J. Huang, and Y. Yang, *Appl. Phys. Lett.* **88**, 253503 (2006).
- ⁶V. Shrotriya, G. Li, Y. Yao, C. W. Chu, and Y. Yang, *Appl. Phys. Lett.* **88**, 073508 (2006).
- ⁷F. J. Zhang, D. W. Zhao, Z. L. Zhuo, H. Wang, Z. Xu, and Y. S. Wang, *Sol. Energy Mater. Sol. Cells* **94**, 2416 (2010).
- ⁸Q. L. Song, M. L. Wang, E. G. Obbard, X. Y. Sun, X. M. Ding, X. Y. Hou, and C. M. Li, *Appl. Phys. Lett.* **89**, 251118 (2006).
- ⁹R. Po, C. Carbonera, A. Bernardi, and N. Camaioni, *Energy Environ. Sci.* **4**, 285 (2011).

- ¹⁰S. Kirchmeyer and K. Reuter, *J. Mater. Chem.* **15**, 2077 (2005).
- ¹¹S.-I. Na, S.-S. Kim, J. Jo, and D.-Y. Kim, *Adv. Mater.* **20**, 4061 (2008).
- ¹²Y. H. Kim, C. Sachse, M. L. Machala, C. May, L. Mueller-Meskamp, and K. Leo, *Adv. Funct. Mater.* **21**, 1076 (2011).
- ¹³F. Nickel, A. Puetz, M. Reinhard, H. Do, C. Kayser, A. Colsmann, and U. Lemmer, *Org. Electron.* **11**, 535 (2010).
- ¹⁴M. C. Barr, J. A. Rowehl, R. R. Lunt, J. Xu, A. Wang, C. M. Boyce, S. G. Im, V. Bulović, and K. K. Gleason, *Adv. Mater.* **23**, 3500 (2011).
- ¹⁵A. Gadisa, K. Tvingstedt, S. Admassie, L. Lindell, X. Crispin, M. R. Andersson, W. R. Salaneck, and O. Inganäs, *Synth. Met.* **156**, 1102 (2006).
- ¹⁶B. Winther-Jensen and F. C. Krebs, *Sol. Energy Mater. Sol. Cells* **90**, 123 (2006).
- ¹⁷S. Admassie, F. L. Zhang, A. G. Manoj, M. Svensson, M. R. Andersson, and O. Inganäs, *Sol. Energy Mater. Sol. Cells* **90**, 133 (2006).
- ¹⁸D. A. Rider, B. J. Worfolk, K. D. Harris, A. Lalany, K. Shahbazi, M. D. Fleischauer, M. J. Brett, and J. M. Buriak, *Adv. Funct. Mater.* **20**, 2404 (2010).
- ¹⁹F. L. E. Jakobsson, X. Crispin, L. Lindell, A. Kanciurzevska, M. Fahlman, W. R. Salaneck, and M. Berggren, *Chem. Phys. Lett.* **433**, 110 (2006).
- ²⁰L. Lindell, A. Burquel, F. L. E. Jakobsson, V. Lemaire, M. Berggren, R. Lazzaroni, J. Cornil, W. R. Salaneck, and X. Crispin, *Chem. Mater.* **18**, 4246 (2006).
- ²¹H.-H. Liao, L.-M. Chen, Z. Xu, G. Li, and Y. Yang, *Appl. Phys. Lett.* **92**, 173303 (2008).
- ²²S. G. Im, K. K. Gleason, and E. A. Olivetti, *Appl. Phys. Lett.* **90**, 152112 (2007).
- ²³D. Fujishima, H. Kanno, T. Kinoshita, E. Maruyama, M. Tanaka, M. Shirakawa, and K. Shibata, *Sol. Energy Mater. Sol. Cells* **93**, 1029 (2009).
- ²⁴L. A. A. Pettersson, L. S. Roman, and O. Inganäs, *J. Appl. Phys.* **86**, 487 (1999).
- ²⁵W. Osikowicz, X. Crispin, C. Tengstedt, L. Lindell, T. Kugler, and W. R. Salaneck, *Appl. Phys. Lett.* **85**, 1616 (2004).
- ²⁶J. S. Huang, P. F. Miller, J. S. Wilson, A. J. de Mello, J. C. de Mello, and D. D. C. Bradley, *Adv. Funct. Mater.* **15**, 290 (2005).
- ²⁷J. S. Kim, B. Lagel, E. Moons, N. Johansson, I. D. Baikie, W. R. Salaneck, R. H. Friend, and F. Cacialli, *Synth. Met.* **111**, 311 (2000).
- ²⁸P. R. Brown, R. R. Lunt, N. Zhao, T. P. Osedach, D. D. Wanger, L.-Y. Chang, M. G. Bawendi, and V. Bulović, *Nano Lett.* **11**, 2955 (2011).
- ²⁹J. Meyer, A. Shu, M. Kroeger, and A. Kahn, *Appl. Phys. Lett.* **96**, 13308 (2010).